Chapter 2

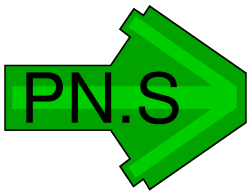

The Planetary Nebula Spectrograph

The Planetary Nebula Spectrograph (PN.S) and the principles of counter-dispersed imaging are described in this chapter. A full description of PN.S, its motivation, design and commissioning can be found in Douglas et al. 2002, *The Planetary Nebula Spectrograph: The Green Light for Galaxy Kinematics*. Other information is also available on the instrument website, www.astro.rug.nl/∼pns.

2.1 Driving forces

As we have discussed in Chapter 1, understanding the kinematics of a galaxy's stellar system is critical to understanding that galaxy's mass profile, and one way stellar kinematics can be measured is by using PNe as a tracer population.

A kinematic survey of PNe using traditional techniques requires two separate observations to be made. The first, an on- off-band imaging survey to search for objects with bright emission lines. These targets are then followed up spectroscopically, usually with a multi-object spectrograph, in order to measure velocities. Surveys of this sort are well established, but require a considerable amount of telescope time.

PN.S, by contrast, was designed specifically for this task and requires only one observation to both detect and measure the velocities of all the PNe in its field of view. As a purpose-built instrument, PN.S has been optimised for this task and makes an efficient use of time, requiring a similar amount of telescope time to the imaging portion of a traditional survey.

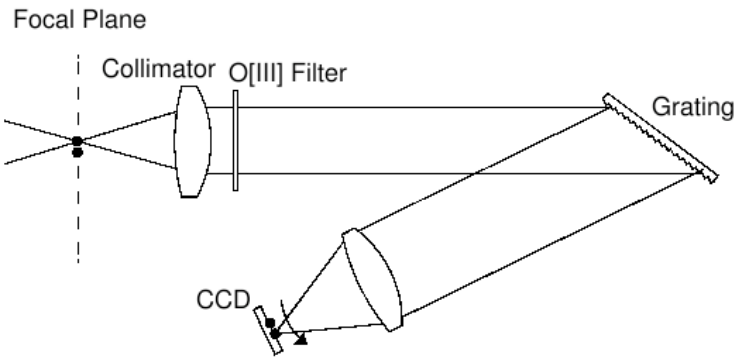

Figure 2.1: Optical setup for counter-dispersed imaging. Light is collimated, passed through a narrow band [O III] filter, dispersed by a grating, then focused onto a CCD.

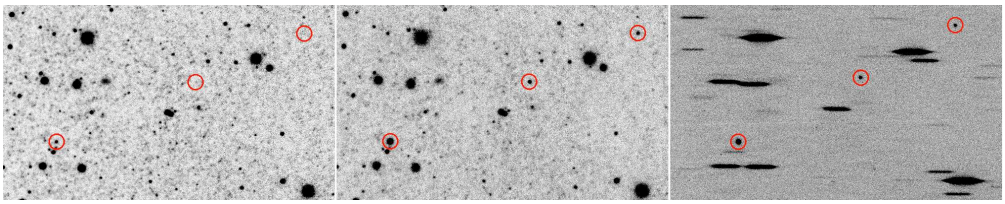

Figure 2.2: Example V-band, narrow band [O III], and PN.S images of the same field (left to right). Locations of the PNe are marked in the three images. In the V-band image the PNe are either not visible or very faint compared to their counterparts in the [O III] narrow band image, while in the PN.S image they are easily identified as the emission line point sources. The V-band and [O III] narrow band images are taken from Massey et al. (2002).

2.2 Counter-dispersed imaging and the PN.S

PN.S works using a technique called counter-dispersed imaging (CDI), a novel application of spectrographic imaging that has its roots in the work of Charles Fehrenbach in the late 1940s (Fehrenbach, 1947, 1948), but was not fully exploited until relatively recently (Douglas & Taylor, 1999). When using CDI to look for PNe, the field of interest is imaged through a narrow band [O III] filter and a slitless spectrograph, as shown in Figure 2.1. In the resulting image, stellar and ambient light is smeared out in the dispersion direction, while the [O III] emission from a PN (or any other ionised gas cloud) remains as a bright point source, as shown in Figure 2.2. PNe are shifted in the dispersion direction away from their true positions by an amount related to the observed wavelength of the emission line.

While it is extremely easy to identify emission line objects in a dispersed image, a single image is of little practical use. In order to extract useful information, a second comparison image is required. This can be a conventional [O III] image allowing comparison against the measured positions, as used by Méndez et al. (2001), but in CDI a second spectrographic image, dispersed in the opposite direction to the first, is used. In PN.S the second, counter-dispersed, image is taken simultaneously with the first by a second spectrograph rotated by 180° as shown in the schematic diagram of the PN.S layout in Figure 2.3. Examining the resulting two images together gives the positions and velocities of any PNe in the field, while photometry can be measured from either

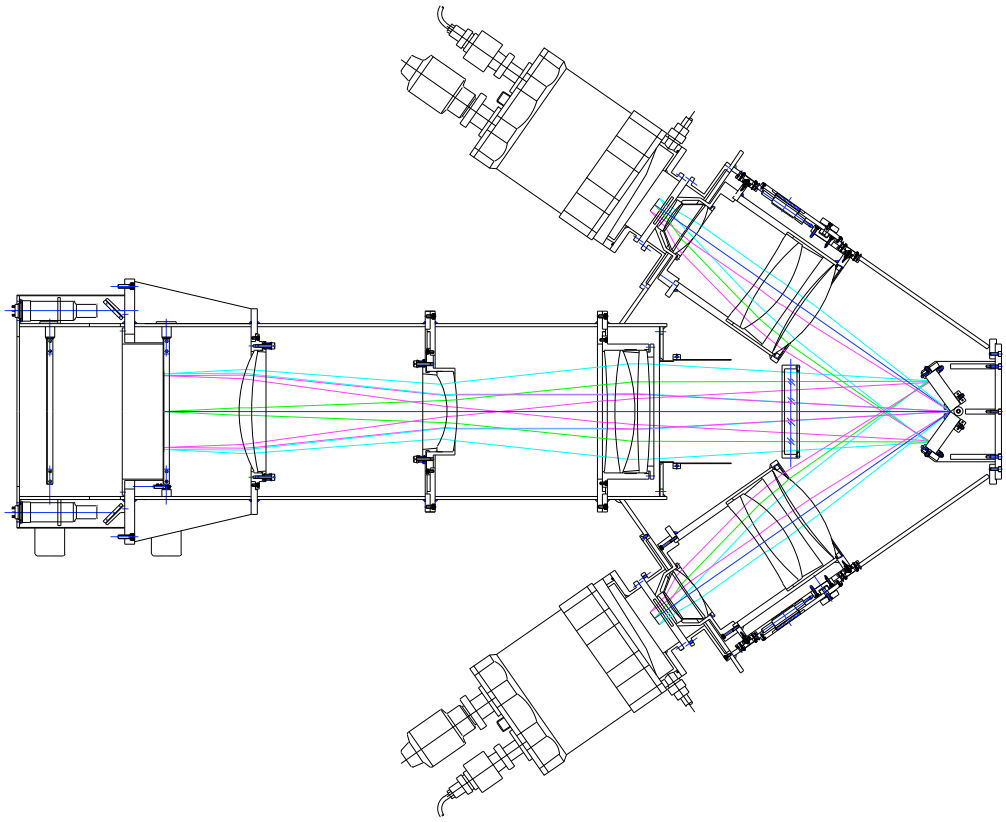

Figure 2.3: A schematic representation of PN.S. The instrument has a pair of gratings at its base (the right hand side of this image) allowing a pair of counter-dispersed images to be produced.

image.

Figure 2.4 shows a small section of the two PN.S images alongside an [O III] image of the same area of sky (Massey et al., 2002). It is readily apparent from the PN.S images which objects are stars and which are PNe. Whilst it is not possible to see the effect of the source velocity on dispersion when looking at individual PNe, we are fortunate in this field to find two PNe that are projected close together but have quite different velocities. These two PNe, located to the centre right of the image, are clearly displaced differently, relative to one another, in the two PN.S images.

2.3 The calibration mask

In practice, turning the PN.S images into useful information requires comparison against calibration images. A calibration mask was therefore built into the instrument, which can be moved into the focal plane by a motor, in between science images. The mask has 178 regularly spaced holes in it (Figure 2.5), through which the telescope's copper-neon-argon arclamps shine 178 short filter-limited spectra (Figure 2.6).

These calibration images are used in two ways. Firstly, the locations of the brightest emission line (5017 Å) are compared to an 'ideal' mask and used to map distortions and

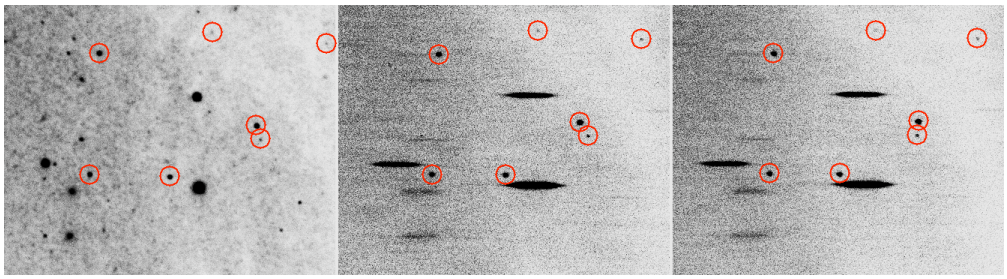

Figure 2.4: An example PN.S image. The left hand image shows a section of one of Massey et al. (2002)'s [O III] images, the middle and right images are the PN.S images of that section of sky. It is readily apparent which of the sources in the [O III] imaging are PNe when compared to the PN.S images and these are highlighted in all three images.

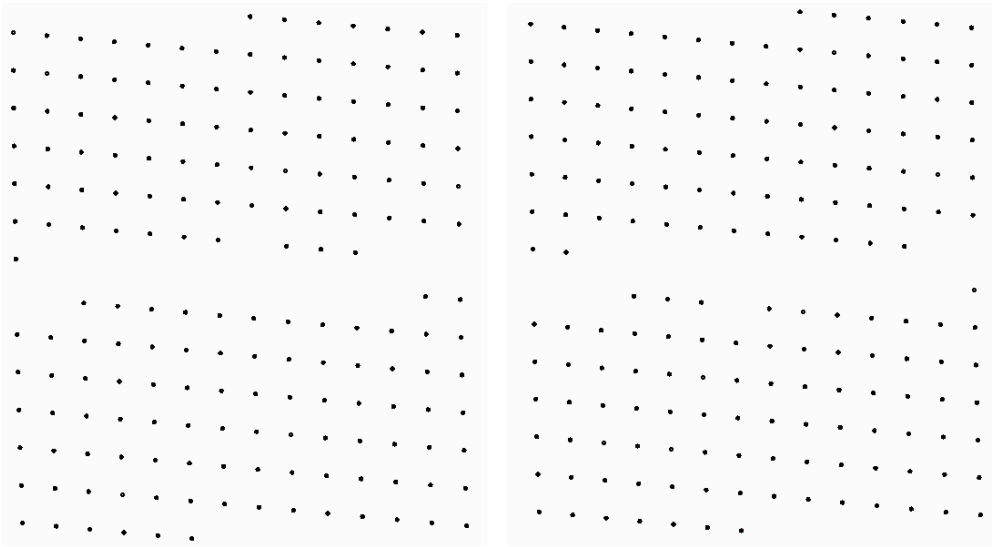

Figure 2.5: Locations of the mask holes as seen in the two PN.S images. For the images to line up one of these must be rotated through $\sim 180°$.

rotations in the calibration images. The maps are then used to remove the distortions in the science images. Secondly, the spectra are used to characterise variations in the dispersion across the image in order to calibrate the PN wavelengths. Use of the calibration masks will be revisited in Chapter 3.

2.4 Instrument specifications

PN.S was designed with three different filters with central wavelengths of approximately 5000 Å, 5034 Å and 5058 Å, giving coverage from the Local Group out to redshift ~ 0.01. The filter mount can be tilted, tuning the filters to the systemic velocity of a target. The filters have very small bandpasses (~ 35 Å) to minimise background noise and reduce the length of stellar trails in the image which can obstruct PN detections. For this survey of the Andromeda Galaxy we use the shortest wavelength filter,

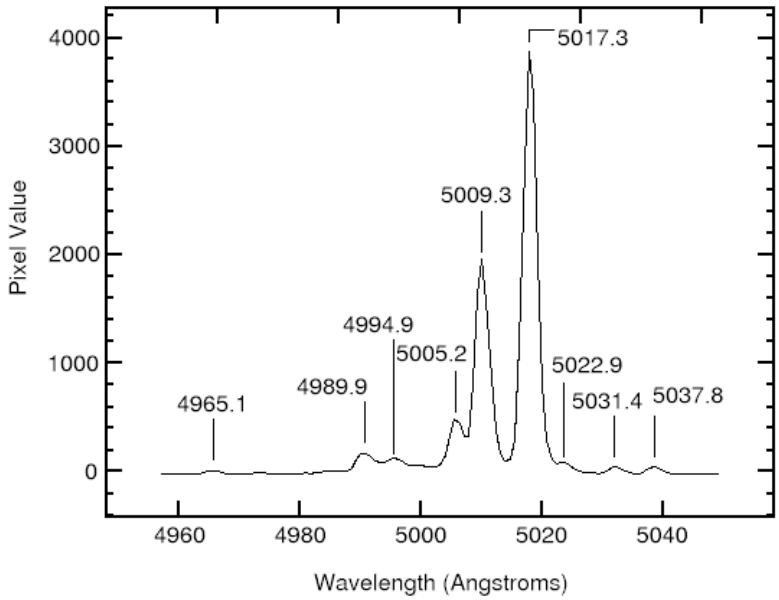

Figure 2.6: Detailed copper-neon-argon arc spectrum seen through filter A set at 0° tilt.

referred to as filter A, configured at 0° tilt. This has a central wavelength of 5002.2 Å and a bandwidth of 36.5 Å, corresponding to a velocity range for the [O III] line of -1380 km s^{-1} to 810 km s^{-1}. This range is well matched to the velocity range of components of M31, which lie between approximately -600 and 0 km s^{-1}, but also allows a significant margin for the detection of any unexpected high-velocity features.

Filter bandwidths of this size are actually rather generous for any individual galaxy, with velocity ranges of ~ 2000 km s^{-1} catered for. Decreasing the bandwidth to around 20 Å would still allow for a 1200 km s^{-1} velocity range, more than sufficient for most galaxies. The resulting reduction in background light, both from the galaxy and the night sky, would improve the overall system efficiency. However, more filters would be required to allow coverage of the same redshift range, and hence number of galaxies, as is allowed by the three filters listed above.

PN.S uses a pair of Spectronic 35-53 600 g/mm, 8.5° blazed gratings to disperse the light. These were chosen to balance the competing needs for small and large dispersions. A small dispersion is needed: to minimise the length of star trails which obliterate a significant fraction of the field; to keep the PNe emission lines within the field of view of both the CCDs; and to minimise the confusion that a large separation between the emission line pairs creates. However, a large dispersion is needed to increase the velocity precision. In the normal setup, these gratings produce dispersions of 1.29 pixels Å^{-1}.

Thus far PN.S has only been used at the William Herschel Telescope, part of the Isaac Newton Group of Telescopes in La Palma (Figure 2.7). We have used a pair of near-identical CCDs belonging to the ING (EEV12 and EEV13) on PN.S's two arms, the basic parameters of which are summarised in Table 2.1. When used with PN.S mounted at the f/10.942 Cassegrain focus, pixel scales of 3.32 pixels per arcsecond in the disper-

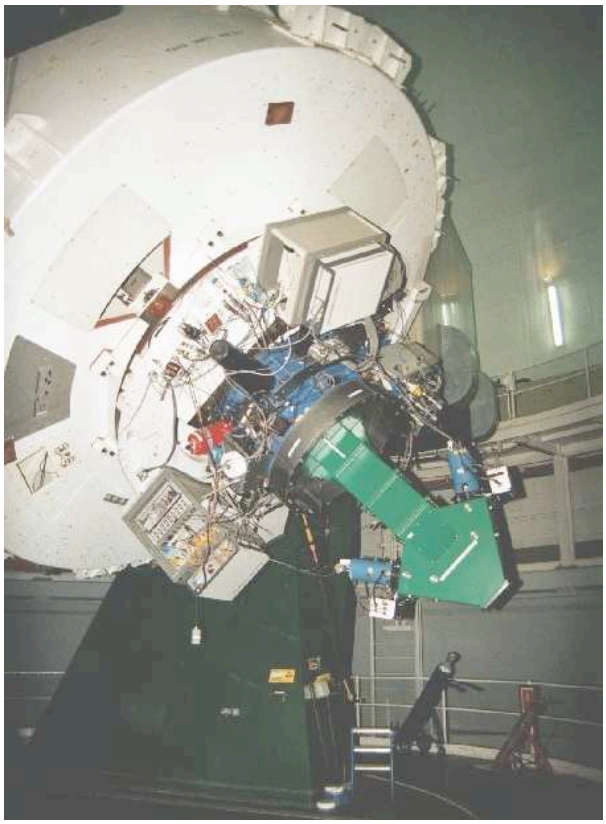

Figure 2.7: PN.S mounted at the Cassegrain focus of the William Herschel Telescope in La Palma.

Table 2.1: CCD Parameters.

	EEV12	EEV13
Pixel size (X×Y)	13.5 × 13.5 μm	13.5 × 13.5 μm
Size of digitised area (X×Y)	2148 × 4200 pixels	2148 × 4200 pixels
Bias (slow readout)	1244 ADU	1060 ADU
Gain	1.16 electrons per ADU	1.20 electrons per ADU
Noise	3.5 electrons	3.6 electrons

sion direction and 3.67 pixels per arcsecond in the spatial direction are obtained. The CCDs are windowed down to 2150 × 2500 pixels, a field size of $10.79' \times 11.35'$. The two images PN.S produces are arbitrarily defined as the left and right hand images. For consistency EEV12 is always used on the left and EEV13 on the right.

2.5 Photometric efficiency

For PN.S to provide a realistic alternative to traditional spectroscopy, it had to be photometrically efficient. The design target was for a total system efficiency of $\sim 30\%$, about twice that of the William Herschel Telescope's Wide Field Fibre Optical Spec-

Table 2.2: Instrumental efficiencies calculated from spectrophotometric standard stars. References: (1) Oke (1974), (2) Oke & Gunn (1983), (3) Oke (1990)

Star	Ref.	F_{5007} (erg s^{-1} Å^{-1})	Date	Efficiency		
				Left	Right	Total
LDS 749B	1	154.759	2002-10-10	0.1424	0.1467	0.2891
BD+33 2642	2	6367.221	2002-10-10	0.1305	0.1322	0.2628
G193-74	3	63.438	2002-10-13	0.1533	0.1393	0.2926
BD+17 4708	3	18303.018	2003-09-29	0.1454	0.1435	0.2890
BD+28 4211	3	8708.624	2002-10-08	0.1365	0.1325	0.2691
BD+28 4211	3	8708.624	2002-10-10	0.1331	0.1290	0.2621
BD+28 4211	3	8708.624	2002-10-11	0.1328	0.1299	0.2626
BD+28 4211	3	8708.624	2002-10-11	0.1322	0.1312	0.2634
BD+28 4211	3	8708.624	2002-10-12	0.1331	0.1298	0.2629
BD+28 4211	3	8708.624	2003-09-29	0.1438	0.1414	0.2852
BD+28 4211	3	8708.624	2003-09-30	0.1371	0.1292	0.2662

trograph (WYFFOS).

We have estimated the total system efficiency for the observational setup described by observing spectrophotometric standard stars. These observations were short ($\sim$ 30 s), and were taken without using the shutter[1]. The flux per unit wavelength was measured from a narrow column through the brightest region of the stellar trail and compared with the published value for this wavelength. As Table 2.2 shows, the total system efficiency estimates are found to be surprisingly consistent, with a mean value of $\mathrm{Eff}_{\mathrm{total}} = 27.3 \pm 0.4\%$, with much of the scatter attributable to the non-photometric conditions. As only a few standard star observations were made during the run this level of consistency may be artificially low. However, since the science goals of this kinematic survey do not require high precision photometry, this uncertainty is of little significance.

2.6 Advantages and disadvantages of PN.S

As has been discussed, PN.S is a photometrically efficient instrument. However, it is not without some drawbacks. The maximum velocity accuracy obtainable is $\sim$ 15 – 20 km s^{-1}, somewhat lower than the $\sim$ 2 – 10 km s^{-1} that can be achieved with traditional spectroscopy (Halliday et al., 2006; Hurley-Keller et al., 2004; Ciardullo et al., 2004). Nevertheless an accuracy of $\sim$ 20 km s^{-1} is sufficient to study even quite subtle kinematic properties of external galaxies.

Apart from the timing efficiency of PN.S's single observation, the instrument has a number of other advantages over traditional techniques, principally, that there is relatively little loss of information. All PNe that are seen in the PN.S images can have velocities measured for them; PNe are only lost if they overlap a stellar trail. With the

[1]The shutter mechanism is slow, taking $\sim$ 10 s to move out and back into the focal plane making timings for short exposures inaccurate. As the CCDs were windowed down, the beginning of the readout was a fast parallel transfer of the charges, creating a fast end to the exposure and improving the accuracy of the timings.

traditional approach, preliminary imaging must be accurate to at least 0.5″ in order to position fibres or slits for follow up spectroscopic observations. Even then, some PNe will not be found. The on- off-band imaging in itself is not foolproof with occasional mis-identifications of continuum objects.

As a new instrument using a relatively untested observing technique, confidence in PN.S's accuracy must be established. As the Andromeda Galaxy has been the subject of a number of recent PN surveys using traditional observing techniques, this survey provides not only the largest survey of PNe in any galaxy but also a unique opportunity to thoroughly test the Planetary Nebula Spectrograph.